

Research Paper

Experimental Investigations to Study the Effectiveness of Cepstral Features to Detect Surface Fatigue Wear Development in a FZG Spur Geared System Subjected to Accelerated Tests

Muniyappa AMARNATH^{(1)*}, I.R. PRAVEEN KRISHNA⁽²⁾, Ramalingam KRISHNAMURTHY⁽³⁾

⁽¹⁾ *Tribology and Machine Dynamics Laboratory, Department of Mechanical Engineering
Indian Institute of Information Technology Design and Manufacturing Jabalpur
Jabalpur 482001, India*

*Corresponding Author e-mail: amarnath.cmy@gmail.com

⁽²⁾ *Department of Aerospace Engineering, Indian Institute of Space Science and Technology
Thiruvananthapuram – 695547, India*

⁽³⁾ *Department of Mechanical Engineering, Indian Institute of Technology
Madras 600025, Tamilnadu, India*

(received December 12, 2019; accepted February 25, 2021)

Gears are essential machine elements used to transmit power and motion from one unit to another under desired angular velocity ratio. Various types of gears have been developed to fulfill power transmission requirements in industrial applications. Under normal or fluctuating operating conditions, increase in fatigue load cycles, transition in lubrication regimes, fluctuating loads and speeds, etc., result in various surface fatigue wear modes which affect the performance of geared system. The severity of wear anomalies developed on gear tooth surfaces can be assessed by using vibration signals acquired from the gear box. On the other hand, reliable wear assessment is very important to perform maintenance action which depends on the sensors, data acquisition procedure, vibration signal analysis and interpretation. This paper presents results of the experimental investigations carried out to assess initiation and propagation of surface fatigue failure wear modes developed on gear tooth contact surfaces. A FZG back to back power recirculation type spur gearbox was used to conduct fatigue test experiments on spur gears under accelerated test conditions. Accelerated test conditions resulted in a rapid transition of lubrication regimes, i.e., hydrodynamic lubrication regime to boundary lubrication regime which triggered surface fatigue faults on gear tooth surfaces. A cepstral analysis method was used to assess fault severity in the geared system. The results obtained from the cepstral features were correlated to various surface fatigue faults and reduction in gear tooth stiffness. Results obtained from the experimental investigations highlighted the suitability of cepstral features to assess incipient faults developed on spur gear tooth surfaces.

Keywords: spur gear; cepstrum; stiffness; pitting; wear.



Copyright © 2021 M. Amarnath *et al.*

This is an open-access article distributed under the terms of the Creative Commons Attribution-ShareAlike 4.0 International (CC BY-SA 4.0 <https://creativecommons.org/licenses/by-sa/4.0/>) which permits use, distribution, and reproduction in any medium, provided that the article is properly cited, the use is non-commercial, and no modifications or adaptations are made.

Nomenclature

a_g – half of the dynamic distance between two suspended teeth,
 E_1, E_2 – modulus of elasticity for gear and pinion respectively,
 E' – combined Young's modulus,
 F – normal tooth force,
 F_U – peripheral tooth force,
 h_d – tooth thickness at the root,
 h_t – tooth thickness at the tip,

I_g, I_f – mass moment inertia of the gear and frame,
 I_i – second moment of area,
 k_1, k_2, k_s – equivalent translational spring effects of the two points of suspension,
 k_{con} – contact stiffness,
 k_{t1} – single tooth stiffness,
 k_{tor} – torsion spring effects of the two points of suspension,
 L_t – tooth length,
 M – torque,

- M_i, M_{i+1} – bending moments acting on x_i and x_{i+1} ,
- S_i, S_{i+1} – slopes at points x_i and x_{i+1} ,
- u – peripheral velocity,
- V – shear force,
- W – load transmitted,
- W_r, W_t – radial and tangential components of gear load W ,
- w – normal tooth force per unit width,
- $X_g(t)$ – displacement of gear,
- $X_f(t)$ – displacement of frame,
- $X(t)$ – relative displacement,
- Y_{rim} – rim deformation.

1. Introduction

Gears are critical machine elements used in complex machinery which transmit power and motion from one shaft to another in desired speed ratios. Condition monitoring of industrial gear transmission play an important role in engineering maintenance in many industries, viz. mining, petroleum refinery, aviation, power generation, transportation, etc. The majority of powerful rotating machines operate at higher load, speeds, and temperatures. These operating conditions cause a reduction in pitting resistance and bending strength of gear tooth surface, thereby resulting

a negative impact on satisfactory operation of gear transmission system.

Under normal operating conditions, a line contact occurs on the gear teeth contact surface in conjunction with a very small circular or elliptical area. Due to such small contact areas, the shear (Hertzian) stress developed at tooth contact surface area is very high. The maximum shear stress occurs at some distance, i.e., approximately 5–10 μm below the gear teeth surface (FERNANDES, MCDULING, 1997; SUNG *et al.*, 2000). Over a period of time, due to increase in fatigue load cycles and change in operating conditions, the cyclic compressive stresses on gear teeth contacting surfaces cause a variation in elastic and plastic behavior in the near surface material of gear teeth contact zone. Further, internal stress concentration is also developed in the gear teeth contact region, which depends on the microstructure and grain orientation of the gear material.

The increase in number of load cycles in the presence of stress concentration results in surface fatigue wear on gear tooth contact surfaces (SUNG *et al.*, 2000; YESILYURT *et al.*, 2003; ZIARAN, DARULA, 2013). Figure 1 depicts the Stribeck curve often used to un-

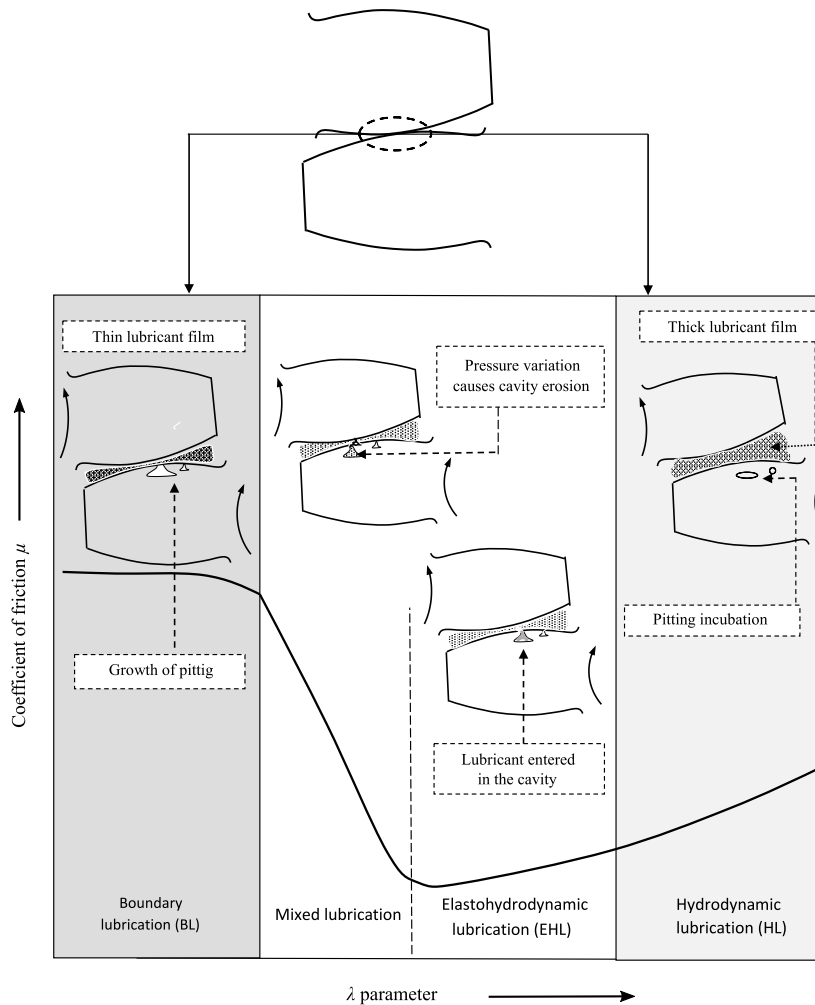


Fig. 1. Pitting incubation and development under various lubrication regimes of Stribeck curve.

derstand the different regimes of lubrication which play a significant role in evaluating the operating performance of lubricated sliding/rolling contact machine elements. These lubrication regimes range from boundary lubrication where metal to metal contact exists to full film or hydro dynamic lubrication in which the metal surfaces are totally separated by a lubricant film. Under normal operating conditions in power/motion transmission, the gear tooth contact surfaces are subjected to fatigue load cycles which trigger a small cavity in the subsurface as shown in the figure. This phase is known as incubation phase, further this cavity develops over a period of time with respect to increase in fatigue cycles, change in operating conditions, viz. breakdown of lubricant film, increase in speeds, fluctuating loads, transition in lubrication regimes, etc. The second phase occurs in EHL and mixed lubrication regime where a capillary is generated which allows the lubricating oil to enter into the cavity (FERNANDES, MCDULING, 1997; FERNANDES, 1996; ZIARAN, DARULA, 2013).

In the third phase, gear teeth meshing action results in a pressure variation in the lubricant entrapped in the pitting cavity. On the other hand, incompressibility of lubricant film between gear teeth leads to cavitation erosion and development of surface fatigue damage in the mixed and boundary lubrication regimes. Figure 1 depicts variation in friction coefficient on gear teeth contact surfaces versus specific film thickness (λ) and their corresponding effects on pitting propagation. The details of ' λ ' estimation by considering geometry, material properties, and operating condition of the geared system are clearly discussed in our previous publications (AMARNATH, LEE, 2015; AMARNATH *et al.*, 2009).

The use of vibration signature analysis for gear fault diagnosis and monitoring has been widely investigated and its application in industry is well established. A gradual increase in vibration levels generally indicates a warning for the growing defects on the rotating machine elements. The machine elements such as gears, bearings, shafts, cams, etc., are often subjected to repetitive load cycles under various operating conditions. Excessive loads, speeds, and improper operating conditions may cause defects on the load bearing surfaces of machine elements, thereby triggering abnormal vibrations in the entire machine structures (ŁAZARZ *et al.*, 2011; WOJNAR *et al.*, 2011). The signal processing techniques are used to analyse time histories and frequency spectra of vibration signals extracted from the machinery.

Numerous research articles available in the literature focus on the analyses of fault related features extracted from time and frequency domain signals to obtain reliable diagnostic information of the defects developed on gear and bearings mounted in the complex rotating machinery (MADEJ *et al.*, 2005; WOJNAR

et al., 2011; ŁAZARZ *et al.*, 2007; WOJNAR, ŁAZARZ, 2007; JACOBSON, 2003; MCFADDEN, 1986; RANDALL, 1982; DALPIAZ *et al.*, 2000).

ZIRAN and DARULA (2013) carried out experimental investigations to assess surface contact fatigue wear in high contact ratio spur gear sets mounted on FZG back-to-back recirculation type spur gearbox. Spectrum and cepstrum analysis methods were used to detect and diagnose distributed faults on gear teeth such as pitting, scuffing, cracks at the tooth root, etc., developed due to surface fatigue wear. The authors have clearly highlighted the wear mechanisms and their severity using gear mesh frequency components and their side bands on both Fourier spectrum and cepstral plots. RANDALL (1982) presented the results obtained from the cepstrum analysis used to monitor and diagnose various classes of gearbox faults. The vibration signals acquired from the gearbox operating under healthy and faulty conditions were processed using Fourier spectrum and cepstrum analyses methods. From these two techniques, cepstrum analysis provided best possibilities of diagnosing the gear faults over a wide range of background conditions.

Results of cepstral plots obtained from the gearbox vibration signals revealed the operating conditions with a minimum knowledge of the detailed dynamic behaviour of individual gearbox. Condition monitoring experiments carried out by DALPIAZ *et al.* (2000) used the cepstrum analysis in conjunction with spectrum, cyclostationary and spectrogram analyses methods to detect simulated faults in the helical gears mounted on a FZG type back-to-back power recirculation type gearbox. The fault detection capabilities of cepstrum analysis of vibration signals were compared to other vibration analysis techniques.

The authors have concluded that the capability of a diagnostic technique depends upon the sensor location, speed, load and type of fault, i.e., local or distributed, and severity of faults. FAKHFAKH *et al.* (2005) carried out numerical and experimental analysis of single stage spur gearbox to quantify presence of distributed and local faults simulated on gear tooth contacting surfaces. Fourier analysis of both experimentally acquired signals and model response provide dependency of mesh frequency on the dynamic behaviour of the geared system.

The cepstrum analysis has the advantages to extract frequencies which indicate the defects and their severity, whereas the results obtained by using Fourier spectrum analysis showed numerous frequency peaks on the spectral plot, which makes it difficult to discriminate fault related spectral features, particularly when the geared system was running under low speeds. EL BADAOUY *et al.* (2001) conducted experimental investigations to highlight the suitability of power cepstrum to detect faults in two stage spur gearbox. The power cepstrum analysis of vibration signals acquired

from the gearbox proved to be the robust detector of faults developed in the geared system running under various operating conditions. The results obtained from this work showed the importance of the cepstrum analysis in which fault related features were found to be independent of signal amplitude, signal-to-noise ratio, and the positions of the sensor.

OZTURK *et al.* (2010) made an attempt at experimentally studying the applications of vibration signal based cepstrum, spectrum, and scalogram analysis methods to detect both local and distributed faults simulated on pitch line zone of the helical gear. The authors concluded that both frequency and cepstrum analyses provided fault diagnostic information in the advanced stage of fault development, whereas mean frequency variation observed in the scalogram analysis was found to be quite useful for detecting faults simulated on gear teeth. PARK *et al.* (2010) introduced a minimum variance cepstrum (MVC) method to detect incipient faults in automotive bearings mounted on an automotive wheel of a car. The authors have considered twelve newly made bearings that passed conventional acceptance test which certified the quality of bearing. These bearings were mounted on an automobile wheel for conducting fault detection experiments.

Minimum variance method was used to crosscheck the quality of bearings which have undergone quality tests. Surprisingly, the MVC method was able to detect incipient faults in four bearings out of twelve, which proved the suitability of this method in bearing fault detection. LIANG *et al.* (2013) considered cepstrum, spectrum, and bispectrum analyses methods to detect the simulated faults in a 2-phase induction motor. The authors have acquired both vibration and current signals to assess the induction motor faults, viz. broken rotor and unsymmetrical stator voltage caused by stator short circuits. The results highlighted the importance of spectrum, cepstrum, and bispectrum analyses for extracting fault related features from vibration and current signals.

However, cepstrum plots obtained from vibration signals were concluded as a too simple approach to assess various faults in induction motor. AMARNATH and LEE (2015) carried out spur gear fatigue test experiments over a period of 1200 hours. The authors have considered both sound and vibration signals in conjunction with tribological parameters to assess wear propagation in the spur geared system. The growth of fault severity on gear teeth contact surfaces was correlated with statistical parameters and spectrum analysis of sound and vibration signals acquired from the gearbox. The surface fatigue wear development on gear teeth contact surfaces was highlighted on gear mesh frequency components. An increase in side bands in conjunction with ghost components was also observed on frequency spectra.

2. Tooth wear, stiffness, and dynamic response of the geared system

Presence of pitting in the gear teeth contact zone causes increase in contact stress, which affects Hertzian compliance around the pitch line. The gear teeth contact is lost due to surface fatigue wear propagation on gear teeth contact region, which results in a gradual reduction of the gear tooth stiffness. The reduction in tooth stiffness causes variations in dynamic behaviour of gear pair, thereby altering vibration/acoustic signals of the geared system (SUNG *et al.*, 2000; YESILYURT *et al.*, 2003). In our previous works (AMARNATH, LEE, 2015; AMARNATH *et al.*, 2009) stiffness modelling and measurement along with spectrum and statistical parameter analyses of vibrations signals were considered to analyse wear in spur geared system. In these works, gear fatigue test experiments were carried out to assess reduction in gear tooth stiffness which occurred due to surface fatigue wear.

A two degree of freedom model based on translation and rotation of gear frame combination was used to measure reduction in stiffness. The results highlighted in (AMARNATH, LEE, 2015; AMARNATH *et al.*, 2009) showed a direct relationship between surface fatigue wear, reduction in stiffness, and increase in vibration amplitudes. Equation (1) is the governing equation used in measurement of reduction in stiffness. Nomenclature gives the details of terms used in the model

$$\begin{bmatrix} M_g & M_f & 0 \\ 0 & I_g & I_f \end{bmatrix} \cdot \begin{Bmatrix} \ddot{x} \\ \ddot{\theta} \end{Bmatrix} + \begin{bmatrix} a^* \\ b^* \end{bmatrix} \cdot \begin{Bmatrix} X \\ \theta \end{Bmatrix} = \begin{Bmatrix} 0 \\ 0 \end{Bmatrix}, \quad (1)$$

where

$$\begin{aligned} a^* &= (M_g + M_f) (k_1 + k_2 + k_3) \\ &\quad - (M_g + M_f) (k_1 a_g - k_2 a_g), \\ b^* &= - (I_g + I_f) (k_1 a_g - k_2 a_g) \\ &\quad - (I_g + I_f) (k_1 a_g^2 - k_2 a_g^2 + k_{\text{tor}} r_t^2). \end{aligned}$$

Figure 2 shows a dynamic model of gear frame combination used for stiffness measurement. The results

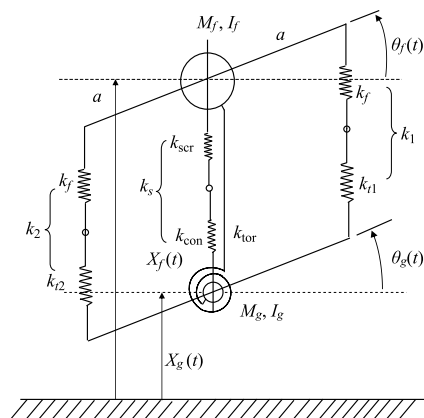


Fig. 2. Dynamic model of gear frame combination.

obtained from the stiffness measurement and corresponding increase in vibration spectrum amplitudes are highlighted in Figs 3a–3d, respectively.

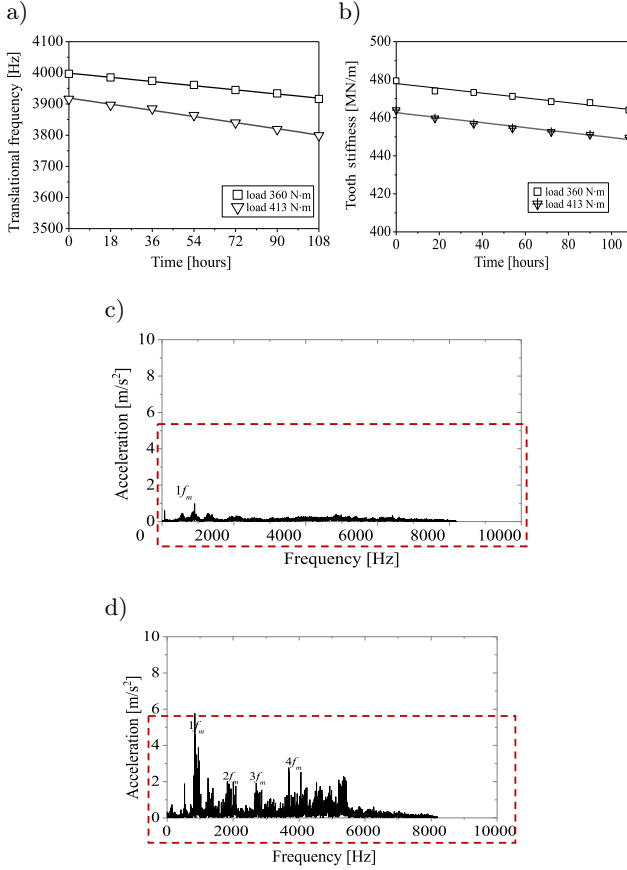


Fig. 3. Change in vibration response of geared system: a) reduction in translational frequency, b) reduction in tooth stiffness, c) frequency spectra of healthy geared system, d) frequency spectra of worn gear (AMARNATH, LEE, 2015; AMARNATH *et al.*, 2009).

The vibration spectra obtained from the experiments consisted of noise and other structural frequency components in the gear mesh frequency regions, as shown in Fig. 3c. Further, the work presented in this paper is carried out in line with our previous works (AMARNATH, LEE, 2015; AMARNATH *et al.*, 2009). Efforts were made to enhance the diagnostic information hidden in the vibration signals acquired from the FZG back-to-back power recirculation type spur gearbox. The cepstrum analysis of vibration signals led to obtain reliable diagnostic features for detecting the growth of surface fatigue wear developed on gear tooth surfaces under accelerated test conditions.

Surface fatigue wear growth on gear tooth contact surfaces has been discussed in detail to correlate reduction in tooth stiffness occurring in the geared system.

The objective of the present work was to accelerate the wear on gear tooth contact surfaces in a short duration, so that the failure can be detected using vibration signal analysis. If the gear pair's design consists

of integral multiple gear teeth (gear teeth with common deviser) the same pair of teeth get engaged in the loading cycle, which accelerates the wear propagation on gear tooth contact surfaces.

3. Cepstrum analysis of vibration signals

The operating conditions of machinery cannot be determined by the frequency analysis alone, since often the changes in the spectrum are masked by noises from the other parts of machinery. The frequency spectrum of vibration signals acquired from complex rotating machinery may not provide reliable diagnostic information due to the changes occurring in the source or transmission path. Hence, it is necessary to use appropriate signal processing method to overcome the aforementioned drawbacks.

A cepstrum can be defined as the Fourier transform of the logarithm of the Fourier transform of a signal, which has been proved to be the promising tool to detect faults in gears and bearings (ZIRAN, DARULA, 2013; FAKHFAKH *et al.*, 2005; LIANG *et al.*, 2013). The most commonly used cepstrums are:

- (i) real spectrum,
- (ii) complex cepstrum,
- (iii) power cepstrum, and
- (iv) phase cepstrum.

The real cepstrum of a signal is given by (DALPIAZ *et al.*, 2000; FAKHFAKH *et al.*, 2005; EL BADAoui *et al.*, 2001; OZTURK *et al.* 2010):

$$c(t) = \frac{1}{2\pi} \int_{-\infty}^{\infty} \log |X| e^{j\omega t} d\omega. \quad (2)$$

The complex cepstrum of a signal $x(t)$ is

$$\check{c}(t) = \frac{1}{2\pi} \int_{-\infty}^{\infty} \log \{X(\omega)\} e^{j\omega t} d\omega. \quad (3)$$

The power cepstrum is given by

$$c(t)^2 = \frac{1}{2\pi} \left[\int_{-\infty}^{\infty} \log |X(\omega)| e^{j\omega t} d\omega \right]^2. \quad (4)$$

The most commonly used cepstrum is power cepstrum of a signal which is successful in detection of surface fatigue faults in rolling/sliding contact machine elements. In vibration signal analysis of complex machinery, cepstrum analysis is used to extract a reliable diagnostic information by identifying a series of harmonics or sidebands in the power cepstrum and their strength. The rhamonics and sidebands in the cepstrum indicate the energy concentration of excitation produced by the rotational component and generally used to detect any abnormalities in the systems operation (ZIRAN, DARULA, 2013; FAKHFAKH *et al.*, 2005; EL BADAoui *et al.*, 2001).

4. Experimental setup and data acquisition procedure

The experimental setup used throughout this work was designed as a FZG back-to-back arrangement and is shown in Fig. 4. This test rig consists of two parallel steel shafts and four gears (two pinions with 25 teeth and the other two gears with 50 teeth); a pair of pinions and gears were mounted on either side of the shafts. The gear sets used in the experiments were made of En 19 steel. The gears with 25 and 50 teeth have a module of 4 mm, pressure angle 20°, and surface roughness in the range of 2–3 μm. In conventional gear test experiments, the torque on gears is applied by external loading, such as Prony brake dynamometer, eddy current dynamometer, a magnetic brake, etc.

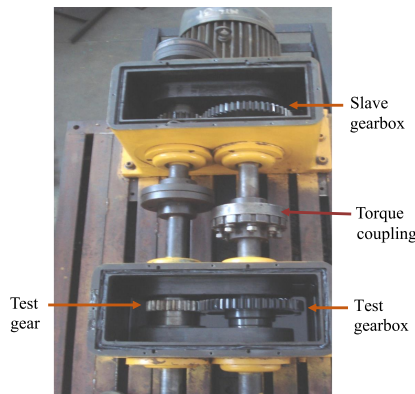


Fig. 4. Standard back-to-back power recirculation gearbox.

In such an arrangement the induction motor has to be carefully controlled for the various shaft speeds under the specified torque. Alternatively, a very simple method may be used to introduce a static torque into the system by using a torque adjustment coupling,

which can provide different levels of torque, according to the relative angle between the two halves of the torque coupling connecting the input shafts.

In the present setup, the torque adjustment coupling connects the two shafts into one axle. The ends of the axle are connected with two pinions, another axle with two gears at the ends is connected to a drive motor. A 10 HP three phase induction motor is used to supply power to the main shaft with a reduction ratio of 1 : 2. The halves of coupling are clamped together in any relative angular position by bolts, the heads of which are located in circular T-Slots in the face of one half coupling. For clamping the coupling, the clamping bolts are released; one half is held stationary by using a clamp and pin, while the other half is acted upon by a large spanner, the applied torque being measured, the coupling is then clamped.

The load applied on the gear sets does not change once the two halves of the torque adjustment coupling are firmly locked in the shaft loop and remains constant for various motor speeds, this being an advantage of utilising this torque coupling method. Further, this arrangement does not need any external load and reduces the complexity of designing the driving system. This has been the most commonly used method to conduct fatigue tests on spur gears. It was ensured that the same pairs of gear teeth were mating after every removal and reassembly during testing.

Alignment of test gears was also maintained throughout the test. In the present experiment, the gearbox was operated at 2100 rpm; eight torque loadings were used: 0, 59, 118, 177, 236, 295, 360, and 413 N·m, the highest value corresponding to a torque of 500% of the rated value to accelerate the wear. Figure 5 shows the gearbox setup with all the measuring instruments. Table 1 summarizes the specifications of the test rig.

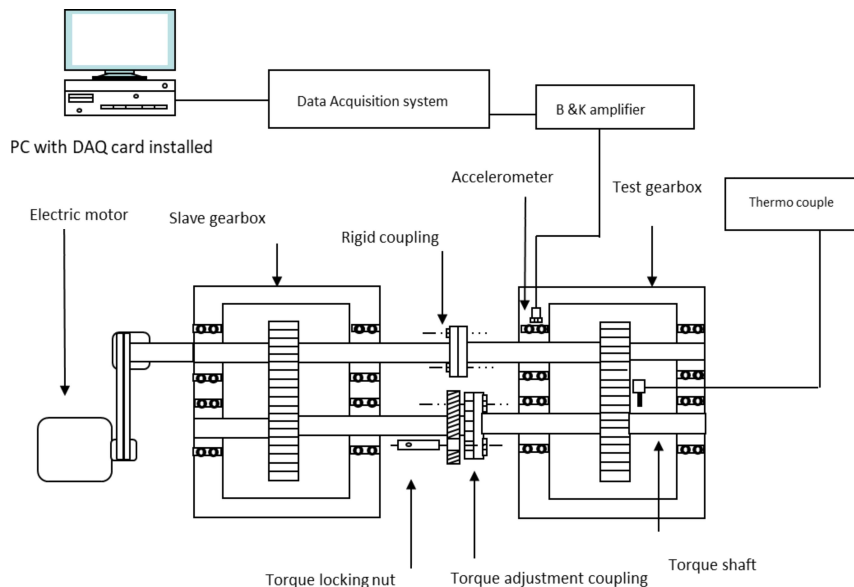


Fig. 5. Gearbox test rig with sensors and instruments.

Table 1. Dimensions and specifications of the test gears.

Pinion gear	
Distance to centre [mm]	150
Pitch diameter	100–200
Module [mm]	4
Number of teeth	25–50
Face width [mm]	25–25
Pressure angle	20°
BHN	130
Material properties of Gears	
Young's modulus	$2 \cdot 10^5 \text{ N/mm}^2$
Poisson's ratio	0.3
Material (steel)	En 19, 0.22% carbon
Shear modulus	$G = 0.8 \cdot 10^5 \text{ N/mm}^2$
Test conditions	
Pinion speed	$n = 2100 \text{ rpm}$
Static load	$W = 0\text{--}690 \text{ N}$
Lever arm	$L = 600 \text{ mm}$
Torque on gear wheel shaft	$0\text{--}413 \text{ N}\cdot\text{m}$

5. Results and discussion

5.1. Wear propagation on gear teeth contact surfaces and correlation to reduction in stiffness and cepstral features

Effective lubrication is critically important because it prevents direct gear tooth contact, reduces friction, prevents high vibration levels, removes heat generated in the geared system. Under typical operating conditions, the lubricant film which separates the gear tooth contacts is very thin, usually of the same order of magnitude as the surface roughness. The changes in operating conditions such as speed, temperature, fluctuating loads, etc., result in breakdown of the lubricant film. This drastic fall in lubricant film thickness leads to gear failures, viz., micro pitting, macro pitting, gear staining, scuffing, and mild wear.

Importance of film thickness and its effects on wear propagation, oxidation of lubricating oil, change in geometry of gear tooth profile, reduction tooth stiffness, variations in sound and vibration levels are vividly discussed in our previous publications (AMARNATH, LEE, 2015; AMARNATH *et al.*, 2009; 2012; LEE, AMARNATH, 2016). Interested readers may refer to these journal articles. As mentioned in the introductory Sec. 1, surface fatigue wear propagation on gear teeth contact region results in gradual reduction in the gear tooth stiffness, which resulted in variations in dynamic behaviour of geared system, thereby altering vibration/acoustic signals.

This section highlights the details of surface fatigue failure modes such as pitting, spalling, scuffing, and

scoring. Gear tooth surfaces were observed with respect to increase in fatigue load cycles. Figure 6 depicts the various forms of surface fatigue failures observed on gear tooth surfaces.

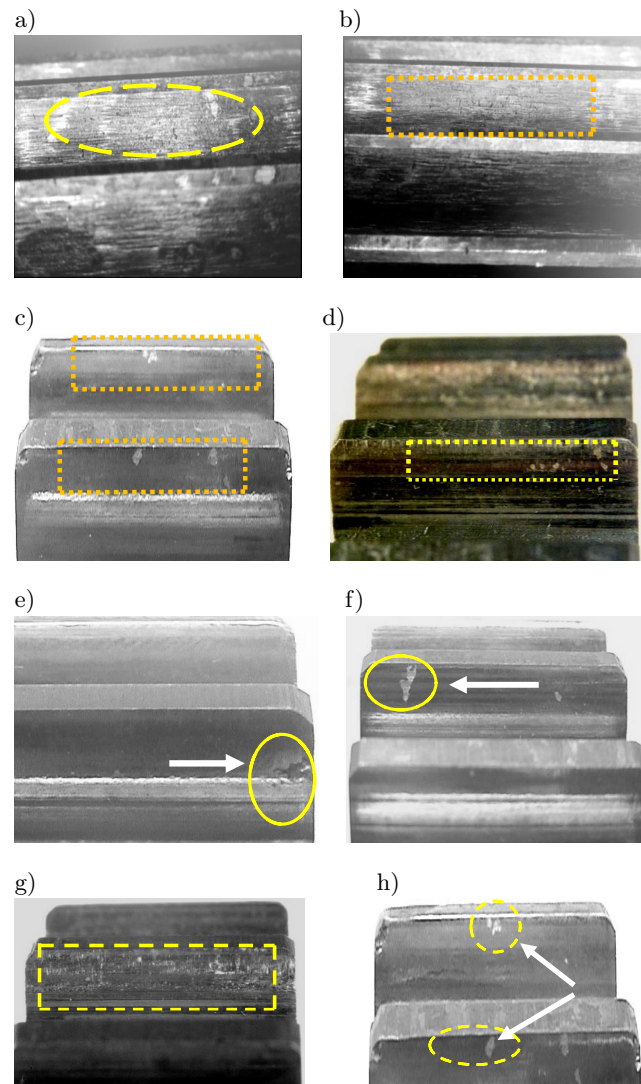


Fig. 6. Surface fatigue wear developed on gear teeth contact under accelerated test conditions: a) initial micro pitting on dedendum after 20 h, b) increase in pit size (after 36 h), c) macro pitting (after 72 h), d) abrasive wear (after 108 h), e) progressive pitting on tooth (after 144 h), e) spalling (after 162 h), f) scuffing (after 198 h), g) increase in pit size (after 216 h).

Micro pitting is a serious form surface fatigue wear which is associated with increase in roughness values occurring under various operating conditions. The pitting is initiated on the surface or subsurface. The surface initiated pitting is a result of increase in surface roughness and poor lubrication between gear teeth contacts, whereas, subsurface pitting is common in a geared system due to subsurface stresses generated in gear tooth contact region even under normal operating conditions with smooth contacts and good lu-

brication (FERNANDES, MCDULING, 1997; FERNANDES, 1996; ZIARAN, DARULA, 2013). Figure 6a depicts surface pitting on gear tooth contacts after 20 hours. This surface fatigue failure may appear anywhere on gear tooth contact surfaces. During power transmission, the sliding and rolling action of both gear and pinion contact surfaces move in the opposite direction, which is considered to be the most critical. This commonly occurs in the dedendum area, hence the surface pitting appeared on the dedendum, as shown in the Fig. 6a. The pitting led to loss of gear accuracy, increase in vibration and noise levels. Increase in pit size, appearance of abrasive wear and progression of pitting is depicted in Figs 6b, 6c, and 6d, respectively.

Lubricant film thickness failure between gear teeth contact leads to spalling, which develops in the vicinity of pitting and propagates in the direction of load moment on the gear tooth flank. Figure 6e depicts spalling developed of gear tooth after 162 hours. Thus, spalling occurring on the gear tooth contact surfaces partially or completely interrupts the elastohydrodynamic action of lubrication thereby causing a significant increase in friction and temperature. On the other hand, stress concentration associated with the spalled tooth contact surfaces result in spreading of the surface fatigue wear on to the adjacent teeth surfaces (FERNANDES, MCDULING, 1997; FERNANDES, 1996; JACOBSON, 2003). Further, prolonged operation under accelerated test conditions, i.e., the torque applied on the pinion was $413 \text{ N} \cdot \text{m}$, which was more than 4–5 times than the allowable torque leading to lubrication film thickness failure.

The scuffing wear appearing on the gear tooth addendum surface as a result of extreme frictional heating is caused by high sliding velocities in conjunction with high stress concentrations. This failure can occur at any stage under normal operating condition of a geared system which can be characterised by solid phase welding and tearing of the affected surface. Normally, the scuffing failure develops on addendum or dedendum where sliding speed reaches to the highest value. Scuffing is also associated with breakdown of lubrication mechanism (FERNANDES, MCDULING, 1997; FERNANDES, 1996). The development of pitting and spalling defects appearing during 20 hours or up to 160 hours cause lack of lubricant replenishment, thereby causing scuffing failure on addendum surface which appeared after 198 hours, as shown in Fig. 6f. The development of abovementioned defects results in a gradual reduction in gear tooth stiffness and altered dynamic response of the geared system. In order to assess the dynamic response of the geared system, the vibration signals were acquired from a pair of perfect teeth after run-in wear test; these signals were considered as base line vibration signature.

The baseline power cepstrum of healthy gear shown in Fig. 7a depicts vibration amplitude $[\text{m}/\text{s}^2]$ on y -axis

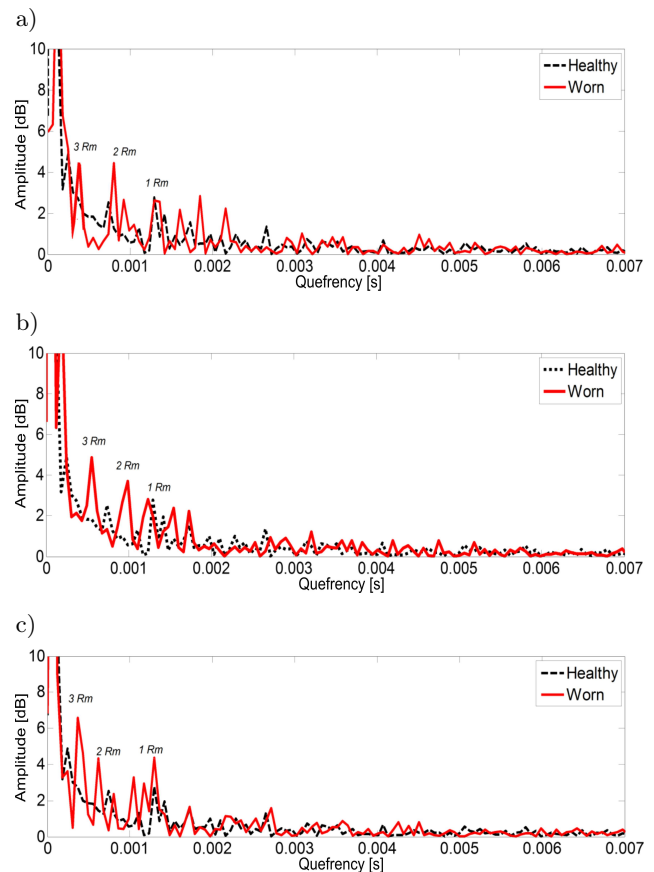


Fig. 7. Cepstral plots obtained under accelerated test 1: a) healthy gear and after 36 h, b) 72 h, c) 108 h.

and quefrency in $[\text{s}]$, i.e., reciprocal of frequency on x -axis. Further, the cepstrum obtained after 32 h of accelerated test 1 is superimposed on the healthy cepstrum. As the surface fatigue wear starts to propagate on the pinion, the first rhamonic (R_m) appearing at a quefrency corresponds to the gear mesh frequency. It is clearly seen in the Fig. 7a that the quefrency corresponding to gear mesh frequency 1.2 ms shows peaks very close to the calculated gear mesh frequency of 875 Hz. The worn gear quefrency peak amplitudes are higher than that of healthy gear quefrency amplitudes. On the other hand, higher quefrency rhamonics of gear mesh frequencies obtained at 0.57 ms and 0.38 ms showed increase in peak values which can be attributed to increase in surface fatigue wear after 32 h. Further, by comparing the cepstral results plotted in Fig. 7a with the spectrum plot shown in Fig. 3b it can be concluded that the cepstrum provided the better diagnostic information in identifying the harmonic or periodicity hidden in the frequency spectra depicted in Fig. 3b. The growth of gear tooth pitting under repeated contact loading result in spalling wear on gear tooth contact surfaces altered the Hertzian compliance, hence the tooth contact is lost. As a result, stiffness between gear teeth is reduced, thereby causing a significant increase in the vibration levels (SUNG

et al., 2000; YESILYURT, *et al.*, 2003). Figure 7b clearly shows a considerable increase in amplitudes of higher rhamonics 2nd R_m and 3rd R_m (higher harmonics) than that of healthy gear cepstrum. The accelerated test 1 was conducted over a period of 106 hours. Prolonged fatigue load cycles led to propagate the pitting wear on gear tooth contact surface in to spalling as highlighted in Fig. 6e, hence the severity of gear defect is revealed in the cepstral plots 7b and 7c where the amplitudes of first three higher cepstral quefrequency rhamonics were observed at 1.2 ms, 0.55 ms, and 0.32 ms, respectively. Further, extended operating cycles and increase in load cycles on the test pinion in accelerated test 2 result in transition of lubrication regimes from elastohydrodynamic to boundary lubrication regime (AMARNATH *et al.*, 2009) during 150–216 h, which resulted in scuffing and increase in pit size on gear teeth contacts. The scuffing wear developed on addendum and dedendum due to lack of lubricant replenishment. In the boundary lubrication regime, the sliding velocities are maximum on addendum and dedendum areas of both pinion and gear, hence the superficial scratches and high polish surface are developed on the gear tooth contact surfaces. As a result, the amplitudes of 1st R_m , 2nd R_m , and 3rd R_m quefrequencies showed a remarkable increase as depicted in Figs 8a–8c.

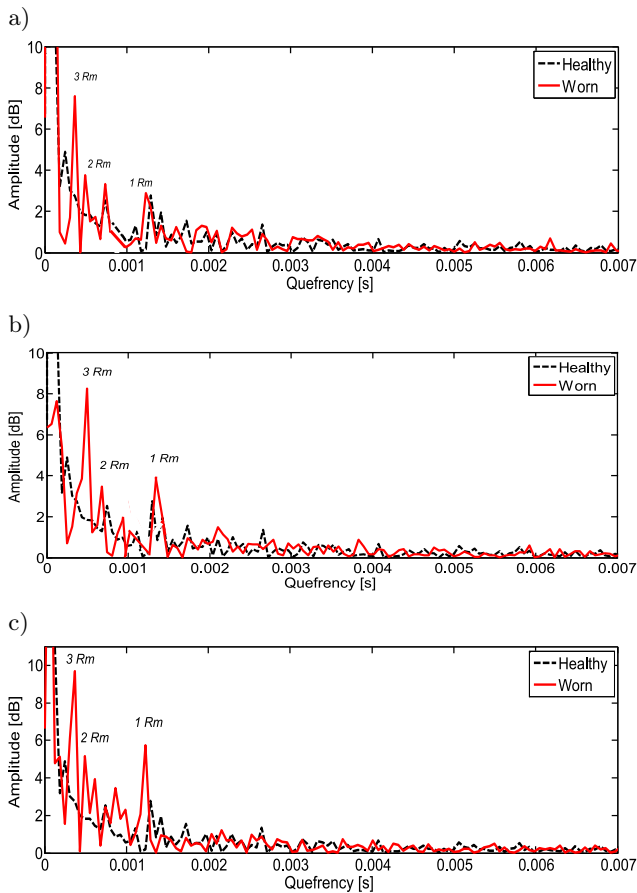


Fig. 8. Cepstral plots obtained under accelerated test 2 for: a) 144 h, b) 180 h, c) 216 h.

The cepstrum analysis provides an advantage such as separation of mixtures of sidebands. On the other hand, one component in the cepstrum represents the global power contents of the whole family of harmonics or sidebands. This value is practically independent of extraneous factors, viz. machine load condition, phasing between amplitude and phase modulation (RANDALL, 1982).

5.2. Correlation between reduction in stiffness and cepstral amplitudes

Further, analysis of cepstral quefrequencies, corresponding harmonic amplitudes provided a better insight to the development of surface fatigue wear. The reduction in tooth stiffness and increase in surface fatigue wear alter the dynamic response of the geared system. Figure 9 depicts quantitative changes of tooth mesh rhamonic amplitudes obtained under accelerated tests 1 and 2 respectively. All the three gear mesh rhamonic amplitudes show the overall increase in trend which can be attributed to wear development on the contacting surfaces. During accelerated test 1, i.e., from 0–108 hours, 2nd and 3rd quefrequency values showed a gradual increase in trend due to increase in surface fatigue wear. Further, during accelerated test 2, the gear pinion undergoing a severe wear caused a significant increase in 1st, 2nd, and 3rd rhamonic quefrequency amplitude values. In order to establish a correlation between wear development, reduction in stiffness, and increase in vibration levels in the geared system the results of stiffness measurement obtained from our previous work (AMARNATH *et al.*, 2012) are shown in Fig. 10 which depicts a gradual reduction in stiffness values plotted on y -axis with respect to increase in fatigue load cycles on x -axis. On the other hand, increase in RMS values which indicate increase in vibration response of the geared system are plotted on the second y -axis in Fig. 10. Mild wear and increase in pit size fault were observed during accelerated test 1 and are shown in Fig. 6b. Due to extended period of operation severe wear faults, viz. spalling abrasive wear marks have been observed on gear tooth surfaces.

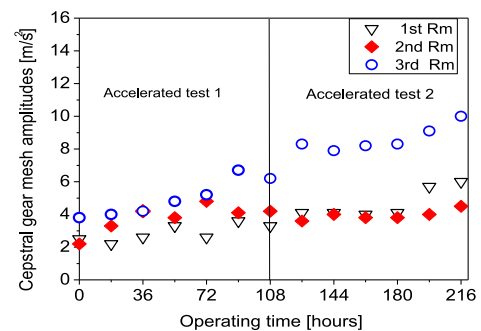


Fig. 9. Amplitudes of harmonics obtained through the accelerated test.

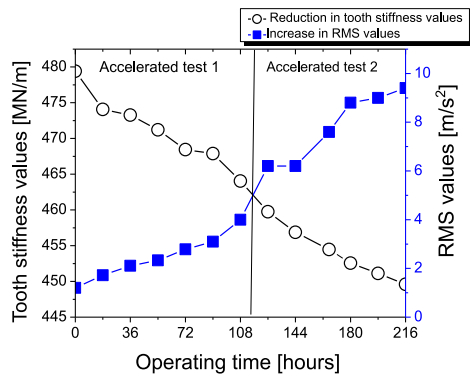


Fig. 10. Reduction in tooth stiffness *versus* increase in acceleration levels obtained under accelerated tests.

For a new pinion the tooth stiffness value of 464 MN/m was obtained. On the other hand, the stiffness value obtained for the same pinion subjected to accelerated tests was 449.6 MN/m. A significant reduction in gear tooth stiffness was observed due to surface fatigue wear. The gear tooth stiffness modelling and measurement work discussed in (AMARNATH *et al.*, 2012) considers a gear frame combination; the translational and rotational frequencies of the gear frame combination were obtained by using experimental modal analysis. A two degree of freedom model of gear frame combination was also used to validate the experimental results. This model considers gear geometry, frame geometry, allowable load, and deflection of the geared system. Interested readers may refer to our publication (AMARNATH *et al.*, 2012) for more details on tooth stiffness reduction measurement procedure.

6. Summary and conclusions

Experimental investigations have been carried out on FZG back-to-back power recirculation type spur gearbox for effective assessment of surface fatigue wear developed on gear tooth contact surfaces under accelerated test conditions. The results presented in this work correlate the surface fatigue wear that appeared on the gear teeth to the reduction in tooth stiffness and increase in the vibration levels of the spur geared system. The following conclusions were drawn from the experimental investigations:

- 1) The accelerated loads and increase in fatigue load cycles resulted in a surface fatigue wear on gear tooth contact surfaces in a short duration of 30–40 hours.
- 2) Increase in surface fatigue faults on gear teeth contacts triggered increase in the vibration levels in the geared system.
- 3) The frequency peaks present in the cepstrum plot reveal the gear tooth defect severity, whereas the FFT analysis showed numerous peaks in the frequency domain plot which are hardly discernible.

- 4) The cepstral plots of healthy and worn gears assisted in minimising the spectral smearing and modulation effects in vibration data acquired from the gearbox.
- 5) The cepstral amplitude values and reduction in gear tooth stiffness values provided a better understanding on the dependency of wear and dynamic response of the geared system.

Further, reduction in surface fatigue wear on the gear tooth contact surfaces is also important to enhance the operating performance of gear transmission system. In this context the authors are working on the surface treatment method. Efforts are being made to utilise the applications laser shock peening method to improve the friction and wear properties of gear pair subjected to fatigue load cycles. This work is under way and the results will be considered in the future publications.

References

1. AMARNATH M., CHANDRAMOHAN S., SEETHARAMAN S. (2012), Experimental investigations of surface wear assessment of spur gear teeth, *Journal of Vibration and Control*, **18**(7): 1009–1024, doi: 10.1177/1077546311399947.
2. AMARNATH M., LEE S.K. (2015), Assessment of surface contact fatigue failure in a spur geared system based on the tribological and vibration parameter analysis, *Measurement*, **76**: 32–44, doi: 10.1016/j.measurement.2015.08.020.
3. AMARNATH M., SUJATHA C., SWARNAMANI S. (2009), Experimental studies on the effects of reduction in gear tooth stiffness and lubricant film thickness in a spur geared system, *Tribology International*, **42**(2): 340–352, doi: 10.1016/j.triboint.2008.07.008.
4. DALPIAZ G., RIVOLA A., RUBINI R. (2000), Effectiveness and sensitivity of vibration processing techniques for local fault detection in gears, *Mechanical Systems and Signal Processing*, **14**(3): 387–412, doi: 10.1006/mssp.1999.1294.
5. EL BADAOUI M., ANTONI J., GUILLET F., DANIERE J., VELEX P. (2001), Use of the moving cepstrum integral to detect and localise tooth spalls in gears, *Mechanical Systems and Signal Processing*, **15**(5): 873–885, doi: 10.1006/mssp.2001.1413.
6. FAKHFAKH T., CHAARI F., HADDAR M. (2005), Numerical and experimental analysis of a gear system with teeth defects, *The International Journal of Advanced Manufacturing Technology*, **25**(5–6): 542–550, doi: 10.1007/s00170-003-1830-8.
7. FERNANDES P.J.L. (1996), Tooth bending fatigue failures in gears, *Engineering Failure Analysis*, **3**(3): 219–225, doi: 10.1016/1350-6307(96)00008-8.

8. FERNANDES P.J.L., MCDULING C. (1997), Surface contact fatigue failures in gears, *Engineering Failure Analysis*, **4**(2): 99–107, doi: 10.1016/S1350-6307(97)00006-X.
9. JACOBSON B. (2003), The Stribeck memorial lecture, *Tribology International*, **36**(11): 781–789, doi: 10.1016/S0301-679X(03)00094-X.
10. LEE S.K., AMARNATH M. (2016), Experimental investigations to establish correlation between stribeck curve, specific film thickness and statistical parameters of vibration and sound signals in a spur gear system, *Journal of Vibration and Control*, **22**(6): 1667–1681, doi: 10.1177/1077546314544164.
11. LIANG B., IWNICKI S.D., ZHAO Y. (2013), Application of power spectrum, cepstrum, higher order spectrum and neural network analyses for induction motor fault diagnosis, *Mechanical Systems and Signal Processing*, **39**(1–2): 342–360, doi: 10.1016/j.ymssp.2013.02.016.
12. ŁAZARZ B., WOJNAR G., CZECH P. (2011), Early fault detection of toothed gear in exploitation conditions, *Maintenance and Reliability*, **2011**(1): 68–77.
13. ŁAZARZ B., WOJNAR G., FIGLUS T. (2007), Comparison of the efficiency of selected vibration measures used in the diagnosis of complex cases of tooth gear damage, *Diagnostyka*, **44**: 19–24.
14. MADEJ H., ŁAZARZ B., WOJNAR G. (2005), Gear-tooth pitting detection through use of the wavelet transform. Tribosysteme in der Fahrzeugtechnik, *Symposium 2005 der Österreichischen Tribologischen Gesellschaft*, Wien, 10 November 2005, pp. 241–248.
15. MCFADDEN P.D. (1986), Detecting fatigue cracks in gears by amplitude and phase demodulation of the meshing vibration, *Journal of Vibration, Acoustics, Stress, and Reliability in Design*, **108**(2): 165–170, doi: 10.1115/1.3269317.
16. OZTURK H., YESILYURT I., SABUNCU M. (2010), Detection and advancement monitoring of distributed pitting failure in gears, *Journal of Nondestructive Evaluation*, **29**(2): 63–73, doi: 10.1007/s10921-010-0066-4.
17. PARK C.S., CHOI Y.C., KIM Y.H. (2013), Early fault detection in automotive ball bearings using the minimum variance cepstrum, *Mechanical Systems and Signal Processing*, **38**(2): 534–548, doi: 10.1016/j.ymssp.2013.02.017.
18. RANDALL R.B. (1982), A new method of modeling gear faults, *Journal of Mechanical Design*, **104**(2): 259–267, doi: 10.1115/1.3256334.
19. SUNG C.K., TAI H.M., CHEN C.W. (2000), Locating defects of a gear system by the technique of wavelet transform, *Mechanism and Machine Theory*, **35**(8): 1169–1182, doi: 10.1016/S0094-114X(99)00045-2.
20. WOJNAR G., ŁAZARZ B. (2007), Averaging of the vibration signal with the synchronizing impulse location correction in tooth gear diagnostics, *Diagnostyka*, **44**: 19–24.
21. YESILYURT I., GU F., BALL A.D. (2003), Gear tooth stiffness reduction measurement using modal analysis and its use in wear fault severity assessment of spur gears, *NDT & E International*, **36**(5): 357–372, doi: 10.1016/S0963-8695(03)00011-2.
22. ZIARAN S., DARULA R. (2013), Determination of the state of wear of high contact ratio gear sets by means of spectrum and cepstrum analysis, *Journal of Vibration and Acoustics*, **135**(2): 021008, doi: 10.1115/1.4023208.